Structures of tetrathiabenzoquinone derivatives and the order–disorder phase transition

Shinya Matsumoto* and Jin Mizuguchi

Department of Applied Physics, Faculty of Engineering, Yokohama National University, 79-5 Tokiwadai, Hodogaya-ku, 240-8501 Yokohama, Japan

Correspondence e-mail: d98jb015@ynu.ac.jp

The tetrathiabenzoquinone derivatives 2,3,7,8-tetrahydro-benzo[1,2-b:4,5-b']bis[1,4]dithiin-5,10-dione (1), $C_{10}H_8O_2S_4$, and 3,4,9,10-tetrahydro-2H,8H-benzo[1,2-b:4,5-b']bis[1,4]di-thiepin-6,12-dione (2), $C_{12}H_{12}O_2S_4$, have attracted attention as new organic pigments. Compound (1) has also been known to exhibit a large third-order non-linear susceptibility. In order to study the electronic structure in the solid state, the crystal structure has been investigated. Compound (1) was found to possess two crystal phases. Phase I is a room-temperature phase in which the molecular conformation is disordered. The other phase II is an ordered phase found at 223 K. Compound (2) is found to be isomorphous with (1) (phase II). Both (1) and (2) form characteristic one-dimensional molecular columns along the stacking c axis and two-dimensional or *quasi* two-dimensional molecular sheets parallel to the *ab* plane. Several close van der Waals contacts were observed between the neighboring molecules. Compound (1) was also found to undergo a reversible order–disorder phase transition at *ca* 265–269 K by X-ray diffraction as well as differential scanning calorimetry.

1. Introduction

Tetrathiabenzoquinone derivatives (1) and (2)

(1)　　　　　　　　(2)
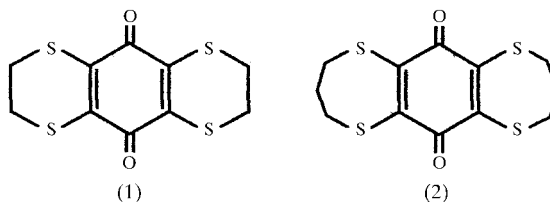
are composed of the benzoquinone group as the chromophore, and the S atoms and the carbonyl groups as the donor and the acceptor, respectively. These dyes form a typical cross-conjugation system. Compounds (1) and (2) have attracted attention as a new organic red and orange pigment, respectively, because of the poor solubility in various organic solvents as well as the vivid coloration in the solid state (Takagi *et al.*, 1998). Compound (1) has also been known to exhibit a large third-order non-linear susceptibility (Matsuoka *et al.*, 1995). Compound (1) is characterized by an extremely large bathochromic shift by *ca* 6600 cm^{-1} on going from solution to the solid state. The energy displacement of the bathochromic shift upon crystallization depends considerably on the side chain group, although no significant difference is recognized in their solution spectra. The bathochromic shift of (2) (*ca* 2100 cm^{-1}) corresponds to only approximately one-third of that of (1).

The bathochromic shift upon crystallization of conventional organic pigments, such as diketopyrrolopyrroles (Mizuguchi,

Table 1
Experimental details.

	(1) (phase I)	(1) (phase II)	(2)
Crystal data			
Chemical formula	$C_{10}H_8O_2S_4$	$C_{10}H_8O_2S_4$	$C_{12}H_{12}O_2S_4$
Chemical formula weight	288.41	288.41	316.47
Cell setting, space group	Orthorhombic, *Ibam*	Orthorhombic, *Pccn*	Orthorhombic, *Pccn*
a, b, c (Å)	9.441 (2), 16.583 (2), 7.184 (3)	9.401 (4), 16.515 (3), 7.053 (4)	9.758 (2), 16.846 (2), 7.981 (2)
V (Å^3)	1124.8 (5)	1095.0 (8)	1312.0 (3)
Z	4	4	4
D_x (Mg m^{-3})	1.703	1.749	1.602
Radiation type	Mo $K\alpha$	Cu $K\alpha$	Mo $K\alpha$
No. of reflections for cell parameters	22	25	25
θ range (°)	12.5–14.8	23.4–28.1	14.7–15.0
μ (mm^{-1})	0.822	7.811	0.713
Temperature (K)	296 (2)	223 (2)	296 (2)
Crystal form, color	Prismatic, dark red	Prismatic, dark red	Prismatic, dark orange
Crystal size (mm)	$0.250 \times 0.080 \times 0.050$	$0.120 \times 0.090 \times 0.070$	$0.80 \times 0.30 \times 0.150$
Data collection			
Diffractometer	Rigaku AFC-7*R*	Rigaku AFC-7*R*	Rigaku AFC-7*R*
Data collection method	ω–2θ scans	ω–2θ scans	ω–2θ scans
Absorption correction	ψ scans	ψ scans	ψ scans
T_{min}	0.959	0.664	0.836
T_{max}	1.000	1.000	1.000
No. of measured, independent and observed reflections	703, 703, 522	1037, 1037, 729	1510, 1510, 1264
Criterion for observed reflections	$I > 2.0\sigma(I)$	$I > 2.0\sigma(I)$	$I > 2.0\sigma(I)$
θ_{max} (°)	27.49	70.09	27.49
Range of h, k, l	$0 \rightarrow h \rightarrow 12$ $0 \rightarrow k \rightarrow 21$ $0 \rightarrow l \rightarrow 9$	$0 \rightarrow h \rightarrow 11$ $0 \rightarrow k \rightarrow 20$ $0 \rightarrow l \rightarrow 8$	$0 \rightarrow h \rightarrow 12$ $0 \rightarrow k \rightarrow 21$ $0 \rightarrow l \rightarrow 10$
No. and frequency of standard reflections	3, every 150 reflections	3, every 150 reflections	3, every 150 reflections
Intensity decay (%)	0.04	−2.36	−0.13
Refinement			
Refinement on	F	F	F
R, wR, S	0.0293, 0.0501, 1.000	0.0733, 0.1041, 1.491	0.0377, 0.0659, 1.051
No. of reflections and parameters used in refinement	522, 56	729, 73	1264, 107
H-atom treatment	H-atom parameters not refined	H-atom parameters not refined	Only coordinates of H atoms refined
Weighting scheme	$w = 1/[\sigma^2(F_o) + 0.00164|F_o|^2]$	$w = 1/[\sigma^2(F_o) + 0.00384|F_o|^2]$	$w = 1/[\sigma^2(F_o) + 0.00346|F_o|^2]$
$(\Delta/\sigma)_{max}$	0.0050	0.0214	0.0338
$\Delta\rho_{max}, \Delta\rho_{min}$ (e Å^{-3})	0.23, −0.17	0.89, −0.62	0.35, −0.28
Extinction method	Zachariasen (1967) type 2 Gaussian isotropic	None	Zachariasen (1967) type 2 Gaussian isotropic
Extinction coefficient	0.002 (2)	–	0.027 (5)

Computer programs used: *MSC/AFC* (Molecular Structure Corporation, 1996), *TEXSAN* (Molecular Structure Corporation, 1998), *SIR*92 (Altomare *et al.*, 1994).

fore, single-crystal X-ray structure analyses were carried out in order to study their electronic structure in the solid state to understand basically the optical properties as mentioned above. In addition, a reversible order–disorder phase transition at low temperatures of (1) has also been investigated.

2. Experimental

2.1. Sample preparation

Both (1) and (2) were prepared by the reported procedure (Takagi *et al.*, 1998). Single crystals of (1) and (2) were obtained by recrystallization from chloroform and chlorobenzene, respectively, as dark colored prisms. The density was measured using the flotation method in a chloroform/diiodomethane solution.

2.2. Structure analysis

Details of data collection and structure refinement are listed in Table 1.[1] The reflection data were collected on a Rigaku AFC-7*R* four-circle diffractometer at room temperature (296 K) for (1) (phase I) and (2), and at 223 K under cold N_2 gas flow for (1) (phase II). The structures were solved by the direct method *SIR*92 (Altomare *et al.*, 1994) and refined by least-squares calculations. All non-H atoms were refined anisotropically. H atoms for both phases of (1) were located on the calculated positions and not refined. H atoms for (2) were found in the difference Fourier map and only the positional parameters were refined. The

1999) and magnesium phthalocyanine compounds (Endo *et al.*, 1999), has been known to be mainly caused by the interactions between transition moments, termed the exciton coupling effect (Kasha, 1963). Exciton coupling effects significantly depend on the molecular arrangement in the crystalline state. The crystal structure thus forms the basis of the investigation of the electronic structure in the solid state from the standpoint of the interactions between transition moments. There-

systematic absences of the reflection data of (1) (phase I) revealed that there are two possible space groups, *Iba*2 and *Ibam*. The latter one gave more reasonable molecular structure and a more accurate R value than the former one. The R values were 0.047 for *Iba*2 and 0.045 for *Ibam*, respectively, for

[1] Supplementary data for this paper are available from the IUCr electronic archives (Reference: OA0031). Services for accessing these data are described at the back of the journal.

non-H atoms based on the disordered structure described below. Then *Ibam* was adopted. There are four molecules in the unit cell and the molecules occupy the special position (2/*m* site symmetry). Therefore, the refinement was carried out on the assumption that the ethylene chain is disordered in two conformations with 50% occupancy. The *R* value for (1) (phase II) is relatively large in spite of the data collection at low temperature. This is caused by the contribution of the twinned peaks occurring at 223 K. The selected interatomic distances are listed in Table 2. All calculations were performed on a Silicon Graphics Indy R-5000 workstation using the *TEXSAN* program package (Molecular Structure Corporation, 1998).

2.3. Phase transition of (1)

The phase transition behavior of single crystals of (1) was monitored by a Rigaku R-axis IV with an imaging-plate area detector using graphite-monochromated Mo $K\alpha$ radiation ($\lambda = 0.7107$ Å, 12.5 kW h^{-1}) at a temperature interval of 25 K ranged between 223 and 298 K using the cold N$_2$ gas-flow method. The camera length was set to be 110 mm from the crystal. The diffraction images were recorded by an oscillation technique ($\Delta\varphi = 2°$) in two different φ angles (0 and 90°) for 20 min at each temperature. Then the lattice type and parameters were calculated by the real-space-indexing algorithm (Duisenberg, 1992) implemented in the *PROCESS* package

(Rigaku Corporation, 1996) to examine the lattice change depending on the temperature.

The phase transition was also confirmed by differential scanning calorimetric (DSC) measurements. The DSC measurements were carried out on 26.850 mg of single crystals of (1) in an aluminium pan using a Rigaku DSC 8230 differential scanning calorimeter equipped with a cooling unit in the temperature range between 233 and 293 K. Both the cooling and warming rates were controlled to be 10 K min^{-1}. Al$_2$O$_3$ was used as a reference sample.

3. Results and discussion

3.1. Molecular geometry

The molecular conformation of (1) and (2) is depicted in Fig. 1. Since the molecules in (1) (phase I) lie on the special
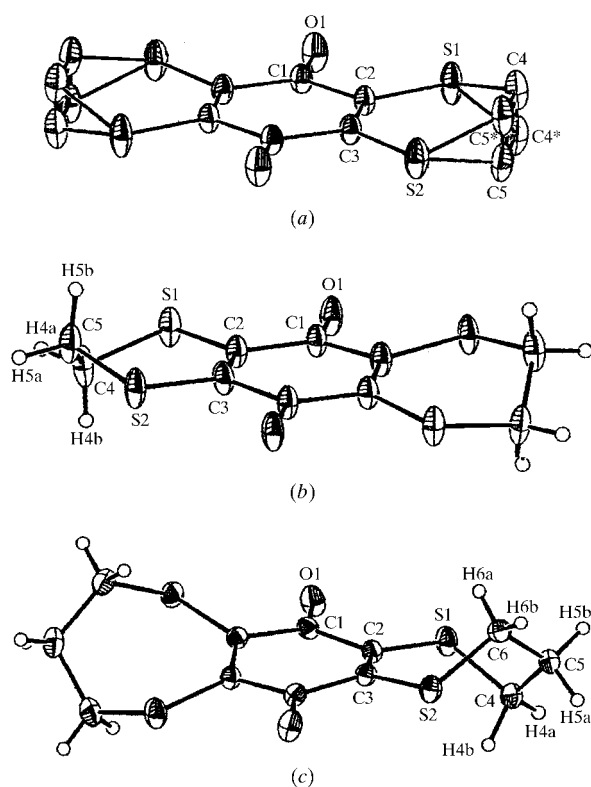
Figure 1
Molecular conformation for (*a*) (1) (phase I), (*b*) (1) (phase II) and (*c*) (2), showing 30% probability level ellipsoids from an *ORTEP*II drawing (Johnson, 1976). H atoms for (1) (phase I) are omitted for clarity. C4* and C5* in (1) (phase I) are disordered atoms whose symmetry codes are: *x*, *y*, −*z*.
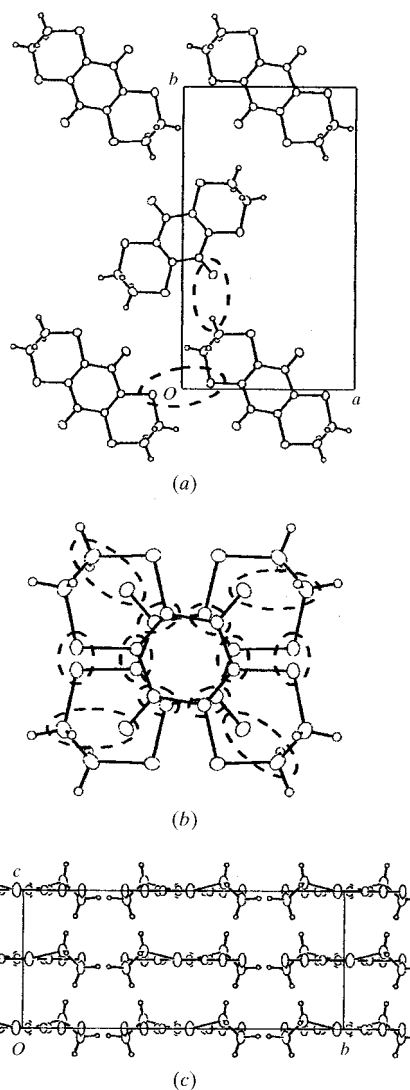
Figure 2
Crystal structure for (1) (phase I), (*a*) a projection onto the *ab* plane, (*b*) the stack pair along the *c* axis and (*c*) a projection onto the *bc* plane. The areas surrounded by the dotted line are designated the close van der Waals contact. The molecules are only depicted in one of the two disordered conformations.

Table 2
Selected interatomic distances for (1) (phase I), (1) (phase II) and (2).

(1) (phase I)		(1) (phase II)		(2)	
Atom pair	Distance (Å)	Atom pair	Distance (Å)	Atom pair	Distance (Å)
S1···S1^i	3.229 (2)	S2···S2^{vi}	3.196 (3)	S1···O1^{xi}	3.807 (2)
S1···S1^{ii}	3.6531 (2)	S2···S2^{vii}	3.5854 (5)	S2···S2^{vii}	3.994 (3)
O1···C4^{iii}	3.631 (5)	O1···C4^{viii}	3.289 (8)	S2···S2^{xii}	3.455 (1)
O1···C5^{iv}	3.321 (4)	O1···C4^{ix}	3.40 (1)	O1···H4a^{viii}	2.80 (3)
O1···C5^v	3.437 (5)	O1···C5^x	3.511 (9)	O1···C6^{xi}	3.452 (3)
O1···H5a^{iv}	2.43	O1···H4a^{viii}	2.41	O1···C4^{viii}	3.452 (3)
C1···C3^{ii}	3.6182 (4)	C1···C2^{ix}	3.542 (9)	O1···C4^{xiii}	3.453 (3)
C2···C2^{ii}	3.6407 (7)	C3···C3^{vii}	3.573 (2)	C1···C2^{xiii}	3.930 (2)
				C3···C3^{vii}	4.0106 (4)

Symmetry codes: (i) $-x, -y, z$; (ii) $x, -y, \frac{1}{2} - z$; (iii) $x, -y, z - \frac{1}{2}$; (iv) $\frac{1}{2} - x, y - \frac{1}{2}, z$; (v) $x, -y, \frac{1}{2} + z$; (vi) $\frac{5}{2} - x, \frac{1}{2} - y, z$; (vii) $x, \frac{1}{2} - y, \frac{1}{2} + z$; (viii) $x - \frac{1}{2}, -y, \frac{1}{2} - z$; (ix) $\frac{3}{2} - x, y, \frac{1}{2} + z$; (x) $\frac{3}{2} - x, y, z - \frac{1}{2}$; (xi) $\frac{1}{2} - x, y, \frac{1}{2} + z$; (xii) $\frac{3}{2} - x, \frac{1}{2} - y, z$; (xiii) $\frac{1}{2} - x, y, z - \frac{1}{2}$.

position (2/m site), the molecular symmetry is D_{2h} to give a completely planar benzoquinone ring together with the disordered ethylene moiety in two conformations with 50% occupancy. On the other hand, the molecular symmetry of isomorphous (1) (phase II) and (2) is C_2 and the benzoquinone ring is not completely planar. The mean deviation at the benzoquinone ring from the least-squares plane for (2) [0.055 (2) Å] is slightly larger than that of (1) (phase II) [0.026 (6) Å] owing to the deformation by the side chain group. The side chain groups of both (1) (phase II) and (2) take the staggered conformation. Bond lengths show no

(a)

(b)
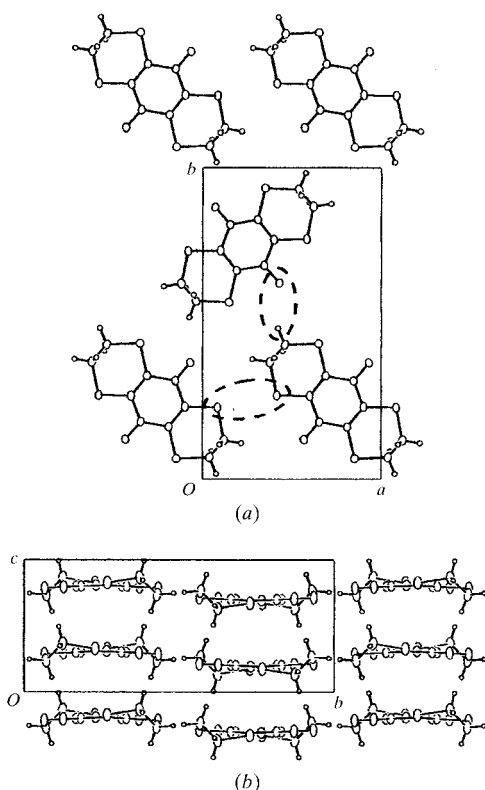
Figure 3
Crystal structure for (1) (phase II), projected onto (a) the ab plane and (b) the bc plane. The areas surrounded by the dotted line are designated the close van der Waals contact.

remarkable difference from the standard value given by Allen et al. (1987).

3.2. Molecular arrangement

In (1) (phase I) the molecules are stacked along the c axis alternatively twisted by approximately 79.5° to give one-dimensional molecular columns, as shown in Figs. 2(a) and (b). The molecules are arranged on a plane parallel to the ab plane, forming a two-dimensional molecular sheet (Fig. 2c). The interplanar distance between the stacking molecules is 3.59 (2) Å. Several close atomic contacts are observed along the stacking direction as described in the next section. The molecules in (1) (phase II) are stacked in the same manner as that in (1) (phase I) and are also arranged in parallel with the ab plane (Fig. 3). The interplanar distance is found to be slightly shorter than that of (1) (phase I) [3.54 (5) Å] mainly due to the thermal motion. The most remarkable difference between the molecular arrangements is that the molecules are either placed on a plane or not. The molecules in the adjacent column along the [110] direction, in which the molecular conformation is inverted, are not on an exact plane, as shown in Fig. 3(b). The molecular plane slightly deviates from the plane in the adjacent column along [110] by approximately 0.71 (5) Å so that the molecules are regarded as forming a quasi two-dimensional molecular sheet.

Molecular arrangement of (2) is almost the same as that of (1) (phase II), as shown in Figs. 4(a) and (b). However, the intermolecular distance is comparatively large [3.98 (9) Å] and the twisted angle between the stacking molecules is relatively acute (70.5°) compared with those of (1) (phase II). The deviation of the molecular plane between the adjacent columns along the [110] direction is also slightly large [1.15 (8) Å]. The difference in the molecular arrangement could be considered as arising from the difference in the side chain group.

3.3. Molecular contact

It should be noted that there are several close van der Waals contacts in these crystals. A relatively short S···S atomic contact of 3.6531 (2) Å in (1) (phase I) and 3.5853 (5) Å in (1) (phase II) are observed between the stacking molecules (Fig. 2b). These atomic contacts are somewhat shorter than the sum of the van der Waals radii (Bondi, 1964). The distance coincides with the value of the typical S···S contact observed in the molecular crystals based on tetrathiafulvalene derivatives for an organic conductor (Leung et al., 1985; Schultz et al., 1986). Although there are several C···O and C···C contacts in the benzoquinone ring, the distance is relatively larger than

the van der Waals contact. The considerably short S···S contact occurs between translationally equivalent molecules along the *a* axis. The distance is 3.229 (2) Å in (1) (phase I) and 3.195 (3) Å in (1) (phase II), respectively. Short atomic contacts between chalcogen atoms have been known to cause extraordinary electronic properties of organic molecular crystals such as tetrathiafulvalene derivatives and so on (Leung *et al.*, 1985; Schultz *et al.*, 1986; Yamashita *et al.*, 1991, 1992). The observed S—S contacts can be considered to influence the extremely large bathochromic shift in (1) in addition to the exciton coupling effects.

Furthermore, there is a CH···O hydrogen bond between the pair with the translationally inequivalent molecules surrounded by the dotted line in Figs. 2(*a*) and 3(*a*). Their C···O, C—H and H···O distances are 3.321 (4), 0.95 and 2.43 Å in (1) (phase I) and 3.289 (8), 0.95 and 2.41 Å in (1) (phase II), respectively. These hydrogen bonds are strong (Steiner, 1997; Desiraju, 1995) and apparently contribute to the formation of the two-dimensional molecular sheet.

On the other hand, atomic contacts in (2) are relatively longer than those in (1). It is mainly due to the effect of the side chain group to enlarge the molecular volume.

3.4. Phase transition in (1)

Single crystals of (1) were found to undergo a reversible order–disordered phase transition at approximately 273 K.
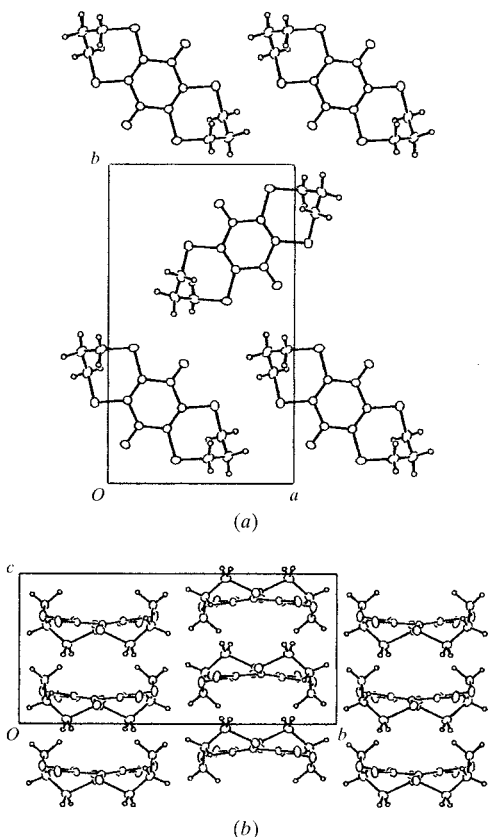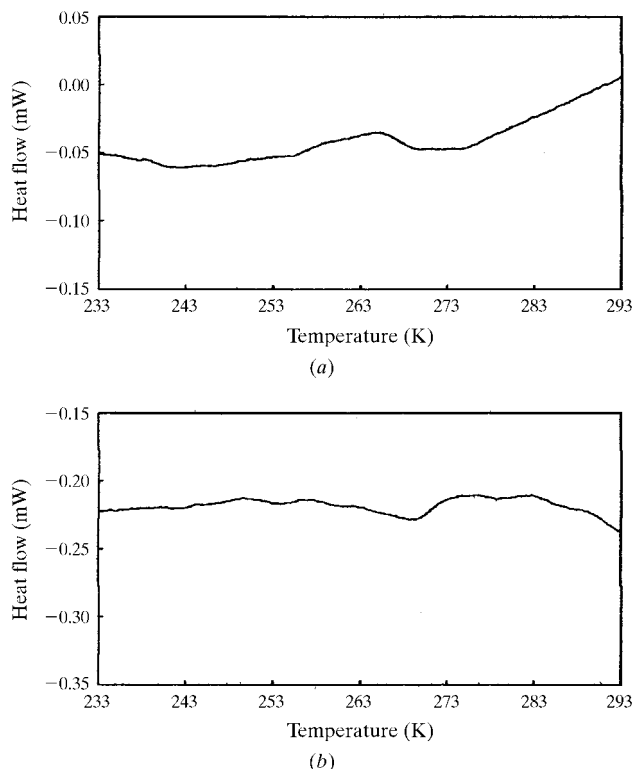

Figure 4
Crystal structure for (2), projected onto (*a*) the *ab* plane and (*b*) the *bc* plane.

The reflection data measured by the imaging plate detector revealed the symmetry of an orthorhombic body-centered lattice at room temperature. However, very weak reflections were recognized at the position of the systematic absence of the body-centered lattice at 273 K. The intensity of the additional peak became larger on lowering the temperature. The reflection data finally indicated the symmetry of an orthorhombic primitive lattice at 248 K. The resulting reflections disappeared as the temperature was increased to 273 K. Consequently, the symmetry of the reflection peaks again showed an orthorhombic body-centered lattice at room temperature.

The phase transition behavior was also confirmed by DSC measurement. The result is shown in Figs. 5(*a*) and (*b*). A small and broad exothermic peak was clearly observed at around 265 K on cooling. On warming, the corresponding small and broad endothermic peak appeared at around 269 K. This result also suggests that the phase transition is reversible.

This phase transition is accompanied by the order–disorder conformational change on the ethylene side chain. This type of phase transition accompanying the change in physical properties such as conductivity, magnetism and so on has been frequently observed in molecular crystals of the compounds containing ethylene side chain groups such as bis(ethylenedithio)tetrathiafulvalene (Leung *et al.*, 1985; Schultz *et al.*, 1986). The influence of the phase transition on the optical properties of (1) will be investigated together with the correlation between the crystal structure and the electronic structure.

Figure 5
DSC curve for (1) between 233 and 293 K (*a*) on cooling and (*b*) on warming.

4. Conclusions

Crystal structures of two tetrathiabenzoquinone derivatives (1) and (2) have been investigated. Conclusions are summarized as follows:

(i) Compounds (1) and (2) form a characteristic one-dimensional column structure along the stacking axis and also form a two-dimensional or a *quasi* two-dimensional molecular sheet parallel to the *ab* plane. The intermolecular distance in (2) is larger than those in (1).

(ii) There are several close interatomic contacts between the chalcogen atoms. The CH···O hydrogen bond was also recognized. The atomic contacts in (1) are closer than those in (2).

(iii) Compound (1) exhibits a reversible order–disorder type phase transition at approximately 265–269 K.

Details of the correlation between the electronic structure in the solid state and the crystal structure will be reported elsewhere (Matsumoto *et al.*, 2000).

References

Allen, F. H., Kennard, O., Watson, D. G., Brammer, L., Orpen, A. G. & Taylor, R. (1987). *J. Chem. Soc. Perkin. Trans. II*, pp. S1–S19.
Altomare, A., Burla, M. C., Camalli, M., Cascarano, M., Giacovazzo, C., Guagliardi, A. & Polidori, G. (1994). *J. Appl. Cryst.* **27**, 435.
Bondi, A. (1964). *J. Phys. Chem.* **68**, 441–451.
Desiraju, G. R. (1995). *Angew. Chem. Int. Ed. Engl.* **34**, 2311–2327.
Duisenberg, A. J. M. (1992). *J. Appl. Cryst.* **25**, 92–96.
Endo, A., Matsumoto, S. & Mizuguchi, J. (1999). *J. Phys. Chem. A*, **103**, 8193–8199.
Johnson, C. K. (1976). *ORTEP*II. Report ORNL-5138. Oak Ridge National Laboratory, Tennessee, USA.
Kasha, M. (1963). *Radiat. Res.* **20**, 55–71.
Leung, P. C. W., Emge, T. J., Beno, M. A., Wang, H. H., Williams, J. M., Petricek, V. & Coppens, P. (1985). *J. Am. Chem. Soc.* **107**, 6184–6191.
Matsumoto, S., Tokunaga, W., Miura, H. & Mizuguchi, J. (2000). *Bull. Chem. Soc. Jpn.* Submitted.
Matsuoka, M., Oshida, A., Mizoguchi, A., Hattori, Y. & Nishimura, A. (1995). *Nonlinear Opt.* **10**, 109–114.
Mizuguchi, J. (1999). *J. Phys. Chem. A*, **104**, 1817–1821.
Molecular Structure Corporation (1996). *MSC/AFC*. MSC, 3200 Research Forest Drive, The Woodlands, TX 77381, USA.
Molecular Structure Corporation (1998). *TEXSAN*. Version 1.9. MSC, 3200 Research Forest Drive, The Woodlands, TX 77381, USA.
Rigaku Corporation (1996). *PROCESS*, Version 4.0. Rigaku Corporation, Tokyo, Japan.
Schultz, A. J., Wang, H. H., Williams, M. & Filhol, A. (1986). *J. Am. Chem. Soc.* **108**, 7853–7855.
Steiner, T. (1997). *Chem. Commun.* pp. 727–734.
Takagi, K., Mizuno, A., Iwamoto, A., Furusyo, M. & Matsuoka, M. (1998). *Dyes Pigments*, **36**, 35–43.
Yamashita, Y., Tanaka, S., Imaeda, K. & Inokuchi, H. (1991). *Chem. Lett.* pp. 1213–1216.
Yamashita, Y., Tanaka, S., Imaeda, K., Inokuchi, H. & Sano, M. (1992). *J. Org. Chem.* **57**, 5517–5522.
Zachariasen, W. H. (1967). *Acta Cryst.* **23**, 558–564.